COBEM 2021 26th International Congress of Mechanical Engineering
November 22-26, 2021, Virtual Congress, Brazil

COB-2021-0574
EXERGETIC ANALYSIS OF AN INTERNAL COMBUSTION ENGINE RUNNING ON E22 AND E100
26th COBEM

Fernando Fusco Rovai
Carlos Eduardo Keutenedjian Mady
Centro Universitário da FEI, Av. Humberto de Alencar Castelo Branco, 3972-B, Assunção, São Bernardo do Campo, São Paulo, Brazil
fusco800@hotmail.com
cekmady@fei.edu.br

Abstract. *The internal combustion engine performance enhancement is a widely explored subject. Additionally to pollutant emissions attention, reducing fuel consumption and consequently the greenhouse gas emissions is one of the leading research and development drivers for the future of the engines industry. As the technologies to increase global engine efficiency are becoming less promising (already reaching improvement limits), the next round would be developing technologies capable of recovering the energy rejected to the environment, especially by cooling and exhaust systems. The internal combustion engine efficiency is mainly assessed by its global efficiency, which consists of an energy balance. The exergy analysis enhances the classic energy analysis from the concept of maximum possible work, including the rejected energy, consisting of a handy tool for the feasibility study of energy recovery systems. This article presents and contrasts the energy and the exergy analyses of a flex-fuel internal combustion engine running on its top global efficiency condition. The boundary fuels are hydrous ethanol (E100) and gasoline blend (E22), available fuels in Brazil. The hydrous ethanol fuel properties (octane number, air-fuel ratio, and vaporization enthalpy) theoretically result in higher energetic engine efficiency than E22 in the same engine hardware, with a fixed compression ratio. Preliminary results of this study point 4,5% higher global engine efficiency running on E100 compared to E22. The higher engine energy efficiency running on E100 than E22 does not happen in the Second Law analysis. The classic exergetic efficiency, based on engine brake power, is similar for E22 and E100. The maximum exergetic efficiency, based on destroyed exergy, is 4,1% higher for E22 compared to E100. The estimation and comparison of the exergy rejected to the cooling and the exhaust systems according to the boundary fuel (about 21 kW on average in this case), is fundamental to assess the potential and the availability of any recovery system eventually implemented in the internal combustion engine.*

Keywords: *flex-fuel engine, waste heat recovery, energy and exergy analysis, hydrous ethanol, gasoline-ethanol blend*

1. INTRODUCTION

Energy conversion efficiency improvement is an important driver for the development of the internal combustion engines. The future of the engines in face of the electrification demands a holistic analysis regarding combustion enhancement, friction reduction and the adoption of energy recovery systems. The engine energy efficiency determined by the First Law can be complemented by the engine exergy efficiency from the Second Law analysis to assess the implementation availability of some energy recovery system especially on exhaust and coolant environment rejections.

The exergetic analysis is being more explored to support the development of new engine technologies. Mahabadipour *et al*. (2019) performed exergetic analysis inside a turbocharged diesel-methane dual fuel engine combustion chamber which resulted about 41 to 42 percent of the total input exergy destroyed due to thermodynamic irreversibilities. Ruffino *et al.* (2019) performed comparative exergetic analysis of gasoline and ethanol blends from combustion heat release inside combustion chamber concluding the exhaust gases are the higher exergy losses and ethanol combustion results less irreversibility than gasoline. Chatzopoulou and Markides (2018) studied the application of an organic Rankine cycle as an engine heat recover increasing the system efficiency by up to 11 percent. The exergetic analysis was applied on experimental data by De Lima *et al.* (2020) to estimate the available energy to be recovered from exhaust gases of an internal combustion engine in different operating conditions analyzing that a 90kW maximum power engine rejected up to 60kW of exergy through exhaust. The feasibility assessment of using an absorption refrigeration system to air-condition the cabin of a urban micro-bus was performed by Ranieri *et al.* (2018) reaching up to 78.9 percent of the vehicle cooling capacity. Özkan (2015) concluded that the injection pressure of a compression ignition engine is inversely proportional to its exergetic efficiency.

The objective of this study is to perform and compare the energetic and the exergetic efficiencies of a spark ignition flex-fuel engine running on Brazilian boundary fuels, hydrous ethanol (E100) and gasoline blend (E22). The main

contribution of this study is to propose and validate a methodology that considers engine non-intrusive experimental data, that does not require the complex combustion chamber instrumentation, obtained in a conventional dyno test bench. This methodology was experimentally validated in a single engine operating condition for both tested fuels providing a comparative energetic and exergetic analyses between E22 and E100.

2. GLOBAL ENGINE THERMODYNAMIC ANALYSIS

2.1 Control volume

The engine control volume adopted in this study is shown in Figure 1, delimited by the dotted line. The inputs considered are fuel and coolant. The outputs are engine effective power, exhaust gases, and coolant. The frontiers of the control volume are the surface of the engine. Therefore, there is no ambition to open toward some aspects of the engine modeling.

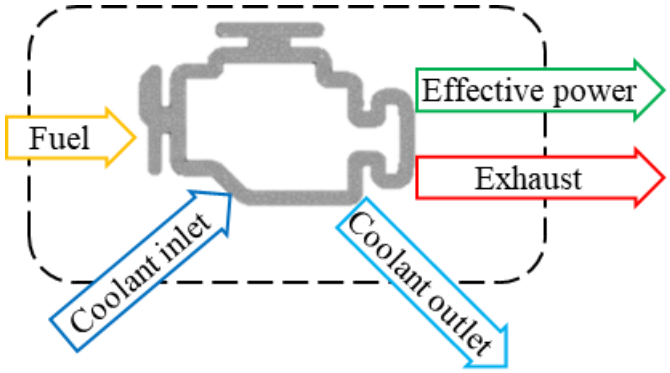

Figure 1. Engine control volume.

A spark ignition, four stroke, flex-fuel, naturally aspirated, multipoint indirect injection engine was tested in a dyno bench at steady-state conditions. This engine was tested running on its two boundary fuels: E22 (gasoline C) and E100 (hydrous ethanol) at the same speed and load conditions, shown in Table 1. This operating point is the highest global efficiency of this engine running on E100.

Table 1. Engine dyno test data. Obtained from: authors.

Fuel		**E22**	**E100**	
Engine speed	n	2500	2500	rpm
Mean effective pressure	BMEP	9.09	9.09	bar
Effective power	$\dot{W}_{eff}$	30.3	30.3	kW
Fuel flow rate	$\dot{m}_{fuel}$	8.300	12.575	kg/h
Lower heating value	LHV	39.26	24.80	MJ/kg
Coolant flow rate	$\dot{m}_{cool}$	0.25	0.25	kg/s
Coolant inlet temperature	T_{in}	60	61	°C
Coolant outlet temperature	T_{out}	88	88	°C
Exhaust temperature	T_{exh}	730	660	°C
Exhaust pressure	P_{exh}	11	10	kPa

2.2 Reference state for the exergy analysis

The exergy analysis requires environmental conditions defined, it is shown in Table 2 (Szargut *et al.*, 1988). Ambient temperature and pressure determine the restrict equilibrium state adopted in thermal and mechanical exergies calculation. The partial pressures of exhaust components are necessary to calculate the chemical exergy and were considered fixed. As the spark ignition engine operates in closed-loop control at stoichiometric air-fuel-ratio the exhaust gases are simplified by a mixture of carbon dioxide, water and nitrogen, hence being possible to use Table 2.

Table 2. Reference ambient conditions (Szargut *et al.*, 1988).

Temperature	T_0	298.15	K
Pressure	P_0	101.325	kPa
Water pressure	$P_{H2O/0}$	2.2	kPa
Oxygen pressure	$P_{O2/0}$	20.39	kPa
Carbon dioxide pressure	$P_{CO2/0}$	0.0335	kPa
Nitrogen pressure	$P_{N2/0}$	75.78	kPa

2.3 Energetic analysis

The energetic analysis of this engine in steady state is carried out by applying the First Thermodynamic Law on the control volume of Figure 1. According to Equation 1, the energy from fuel ($\dot{Q}_{fuel}$) reduced by the energy rejected by cooling ($\dot{Q}_{cool}$), the energy rejected by exhaust ($\dot{Q}_{exh}$) and other power losses from other energy transfer ($\dot{Q}_{loss}$), e.g., friction, noise and auxiliaries, results in engine effective power output ($\dot{W}_{eff}$).

$$\dot{Q}_{fuel} + \dot{Q}_{cool} + \dot{Q}_{exh} + \dot{Q}_{loss} = \dot{W}_{eff} \tag{1}$$

2.4 Exergetic analysis

The rejected energy, calculated from energetic analysis, can be partially recovered up to Carnot's efficiency limit. The maximum recoverable energy can be represented by the property called exergy. The rejected energy impossible to be recovered can be called destroyed exergy ($\dot{B}_d$). The destroyed exergy is determined by Equation 2.

$$\dot{B}_d = \dot{B}_{fuel} + \dot{B}_{cool} + \dot{B}_{exh} - \dot{W}_{eff} \tag{2}$$

The chemical fuel exergy ($\dot{B}_{fuel}$) that is not converted in mechanical energy through engine output is rejected by cooling system ($\dot{B}_{cool}$) and by the exhaust flow ($\dot{B}_{exh}$).

2.5 Fuel energy and exergy

The Brazilian fuels energy can be estimated based on governmental regulations of INMETRO (2008) and ANP (2009, 2015). Complementary fuel properties and the atmospheric air composition are assumed according to Heywood (1988). Gasoline C (E22) is a blend of pure gasoline and 22% anhydrous ethanol by volume. Despite a very small portion of fuel are not burnet the fuel combustion is modelled by complete stoichiometric oxidation. The E22 combustion is represented by Equation 3. Equation 4 represents the complete stoichiometric combustion for hydrous ethanol (E100).

$$C_1H_{2.03}O_{0.078} + 1.4685\,(O_2 + 3.773\,N_2) \rightarrow CO_2 + 1.015\,H_2O + 5.5407\,N_2 \tag{3}$$

$$C_1H_{3.207}O_{0.604} + 1.4998\,(O_2 + 3.773\,N_2) \rightarrow CO_2 + 1.6035\,H_2O + 5.6586\,N_2 \tag{4}$$

Table 3. Fuel energy and exergy flows.

Fuel		**E22**	**E100**	
Air-fuel-ratio	λ	13.259	8.330	
Fuel flow rate	$\dot{m}_{fuel}$	8.300	12.575	kg/h
Lower heating value	LHV	39.26	24.80	MJ/kg
H / C		2.030	3.207	
O / C		0.078	0.604	
β (1)		1.0741	1.1226	
Fuel energy flow rate	$\dot{\mathbf{Q}}_{\mathbf{fuel}}$	**90.51**	**86.63**	**kW**
Fuel exergy flow rate	$\dot{\mathbf{B}}_{\mathbf{fuel}}$	**97.22**	**97.25**	**kW**

(1) Table 3.3 of Szargut *et al.* (1988).

From equations 3 and 4 it is possible to determine the air-fuel-ratio of each fuel. The fuel energy flow (Equation 5) is calculated multiplying the fuel flow and its lower heating value from Table 1. According to Szargut *et al.* (1988), the fuel

exergy is determined by Equation 6 where β coefficient is calculated for liquid fuels composed by carbon, hydrogen and oxygen. These results are shown in Table 3.

$$\dot{Q}_{fuel} = \dot{m}_{fuel} LHV \tag{5}$$

$$\dot{B}_{fuel} = \dot{m}_{fuel} \beta LHV \tag{6}$$

2.6 Coolant energy and exergy

The coolant system heat flow is determined by Equation 7 for coolant inlet ($\dot{Q}_{in}$) and by Equation 8 for coolant outlet ($\dot{Q}_{out}$), where $\dot{m}_{cool}$ is the coolant flow, c_p is the coolant specific heat and T the coolant and ambient temperatures. The coolant specific heat is determined according to Moran *et al*. (2011).

$$\dot{Q}_{in} = \dot{m}_{cool} c_{p,in} (T_{in} - T_0) \tag{7}$$

$$\dot{Q}_{out} = \dot{m}_{cool} c_{p,out} (T_{out} - T_0) \tag{8}$$

The heat rejected to coolant ($\dot{Q}_{cool}$), the difference between outlet and inlet coolant heat flow, is calculated according to Equation 9 and shown in Table 4.

$$\dot{Q}_{cool} = \dot{m}_{cool} \Delta H_{cool} = \dot{Q}_{in} - \dot{Q}_{out} \tag{9}$$

The coolant supplies exergy to engine through inlet boundary at coolant inlet temperature ($\dot{T}_{in}$). The engine rejects exergy through outlet boundary at coolant outlet temperature ($\dot{T}_{out}$). Considering that coolant outlet temperature is higher than inlet, the exergy rejected through coolant is the difference between outlet and inlet exergies. The engine coolant exergy ($\dot{B}_{cool}$) in steady state is calculated by Equation 10 and shown in Table 4.

$$\dot{B}_{cool} = \left[\dot{Q}_{in} \left(1 - \frac{T_0}{T_{in}} \right) - \dot{Q}_{out} \left(1 - \frac{T_0}{T_{out}} \right) \right] \tag{10}$$

Table 4. Coolant energy and exergy flows.

Fuel		**E22**	**E100**	
Engine speed	n	2500	2500	rpm
Mean effective pressure	BMEP	9.09	9.09	bar
Coolant flow rate	$\dot{m}_{cool}$	0.25	0.25	kg/s
Coolant inlet temperature	T_{in}	60	61	°C
Coolant inlet specific heat (1)	$c_{p,in}$	4.186	4.187	kJ/kgK
Coolant outlet temperature	T_{out}	88	88	°C
Coolant outlet specific heat (1)	$c_{p,out}$	4.206	4.206	kJ/kgK
Coolant inlet heat flow rate	$\dot{Q}_{in}$	33.63	37.68	kW
Coolant outlet heat flow rate	$\dot{Q}_{out}$	66.24	66.24	kW
Coolant energy flow rate	$\dot{\mathbf{Q}}_{\mathbf{cool}}$	**-29.61**	**-28.56**	**kW**
Coolant exergy flow rate	$\dot{\mathbf{B}}_{\mathbf{cool}}$	**-7.71**	**-7.50**	**kW**

(1) linear interpolation of Table A-19 from Moran *et al*. (2011).

The engine was tested without thermostat valve and the coolant inlet temperature was adjusted to achieve the same coolant outlet temperature for both fuels. The lower E100 energy rejected though coolant results in lower rejected exergy.

2.7 Exhaust energy and exergy

The exhaust energy flow ($\dot{Q}_{exh}$) of Equation 11 is calculated according to Özkan (2015). Considering that the engine in this study is running on stoichiometric air-fuel mixture, assuming complete combustion the exhaust gases results in a mixture of CO_2, H_2O and N_2 (index i on equations). The mass flow of each exhaust component ($\dot{m}_{exh,i}$) is determined by Equations 3 and 4. The specific heat of each exhaust components ($c_{p,exh,i}$) are calculated according to Moran *et al*. (2011)

based on exhaust temperature of each tested fuel. The ambient reference temperature (T_0) from Table 2 and the exhaust temperature (T_{exh}) shown on Table 5 are considered.

$$\dot{Q}_{exh} = \sum_i \dot{m}_{exh,i}\, c_{p,exh,i}(T_0 - T_{exh}) \tag{11}$$

The exhaust mass flow is determined by the air-fuel ratio (λ) of Equation 12 and by the air and fuel mass balance of Equation 13. The fuel mass flow of each tested fuel is shown in Table 5.

$$\lambda = \frac{\dot{m}_{air}}{\dot{m}_{fuel}} \tag{12}$$

$$\dot{m}_{exh} = \dot{m}_{air} + \dot{m}_{fuel} \tag{13}$$

The exhaust exergy flow ($\dot{B}_{exh}$) is calculated on Equation 14 by the sum of the exergy components: thermal ($b^{th}_{exh,i}$), mechanical ($b^{m}_{exh,i}$) and chemical ($b^{ch}_{exh,i}$).

$$\dot{B}_{exh} = \sum_i \dot{m}_{exh,i}\left(b^{th}_{exh,i} + b^{m}_{exh,i} + b^{ch}_{exh,i}\right) \tag{14}$$

The thermal exergy of each component of exhaust gases (assumed CO_2, H_2O and N_2) is determined by Equation 15 according to Kotas (1985). The enthalpy (h) and entropy (s) of each component of exhaust gases are adopted from Table A-23 of Moran *et al*. (2011) where index $_0$ means ambient reference.

$$b^{th}_{exh,i} = \left(h_i - h_{0,i}\right) - T_0(s_i - s_{0,i}) \tag{15}$$

The exhaust mechanical exergy of Equation 16 considers the constant of the mixture of exhaust gases: CO_2, H_2O and N_2. The exhaust pressure (P_{exh}) are shown in Table 5 and the ambient reference temperature (T_0) and pressure (P_0) are shown in Table 2. The universal gas constant (R) and the molar mass (M) on each component are constants.

$$b^{m}_{exh,i} = T_0 \frac{R}{M_i} \ln\left({}^{P_{exh}}/_{P_o}\right) \tag{16}$$

Table 5. Exhaust energy and exergy flows.

Fuel		**E22**	**E100**	
Engine speed	n	2500	2500	rpm
Mean effective pressure	BMEP	9.09	9.09	bar
Fuel flow rate	$\dot{m}_{fuel}$	8.300	12.575	kg/h
Air-fuel-ratio	λ	13.259	8.330	
Exhaust temperature	T_{exh}	730	660	°C
Exhaust flow rate	$\dot{m}_{exh}$	118.3	117.3	kg/h
Exhaust pressure	P_{exh}	11	10	kPa
Exhaust energy flow rate (1)	$\dot{\mathbf{Q}}_{\mathbf{exh}}$	**-29.56**	**-26.77**	**kW**
Thermal specific exergy	b^{th}_{exh}	-13.45	-11.63	kW
Mechanical specific exergy	b^{m}_{exh}	-0.29	-0.27	kW
Chemical specific exergy	b^{ch}_{exh}	-0.36	-0.37	kW
Exhaust exergy flow rate	$\dot{\mathbf{B}}_{\mathbf{exh}}$	**-14.10**	**-12.27**	**kW**

(1) specific heat from Table A-21 of Moran *et al*. (2011).

The chemical exergy of each exhaust component is determined by Equation 17 according to Kotas (1985). The first term of Equation 17 estimates the chemical exergy of each exhaust component, and the second term estimates the effect of the mixture of the exhaust gases on chemical exergy. The chemical exergy values of each gas component ($b_{q,i}$) were extracted from Table A-26 Model II of Moran *et al*. (2011) and weighted by its molar fraction (y_i).

$$b_{exh,i}^{ch} = \frac{1}{M_i}\left[y_i b_{q,i} + T_0 R y_i \ln(y_i)\right] \quad (17)$$

The lower exhaust temperature with E100 is theoretically expected and experimentally verified by the higher engine efficiency on E100. The lower exhaust pressure with E100 is explained by the lower exhaust flow.

2.8 Effective power

The engine effective power is measured in engine output axle coupled to a dynamometer test bench. The effective power represents the difference between the indicted power and the friction power. The indicated power is a result of the fuel combustion inside the combustion chamber. The friction power represents the power transport losses from combustion chamber through engine output axle. In this case of alternative engine, the friction losses include crank-rod mechanism and auxiliary components.

The exergetic efficiency comparison between tested fuels is performed, as closest as possible, at the same engine condition achieved by constant engine speed and mean effective pressure. The effective power results are summarized in Table 6.

Table 6. Effective power measurement.

Fuel		**E22**	**E100**	
Engine speed	n	2500	2500	rpm
Mean effective pressure	BMEP	9.09	9.09	bar
Effective power	$\dot{\mathbf{W}}_{\mathbf{eff}}$	**30.3**	**30.3**	**kW**

3. RESULTS AND DISCUSSION

The main objective of this study is the comparison of the engine energetic efficiency, usually considered for internal combustion engines, and the exergetic efficiency which is a relatively more recent concept.

3.1 Energetic efficiency

The first verification of this study is the validity of the First Thermodynamic Law, enunciated by Equation 1, to determine the power losses ($\dot{Q}_{loss}$), e.g., friction, noise and auxiliaries. These values are presented in Table 7.

Table 7. Energy balance.

Fuel		**E22**	**E100**	
Engine speed	n	2500	2500	rpm
Mean effective pressure	BMEP	9.09	9.09	bar
Fuel energy flow rate	$\dot{Q}_{fuel}$	90.51	86.63	kW
Coolant energy flow rate	$\dot{Q}_{cool}$	-29.61	-28.56	kW
Exhaust energy flow rate	$\dot{Q}_{exh}$	-29.56	-26.77	kW
Effective power	$\dot{W}_{eff}$	30.3	30.3	kW
Power losses	$\dot{\boldsymbol{Q}}_{\boldsymbol{loss}}$	**-1.04**	**-1.00**	**kW**

From Table 7 the power losses can be considered similar for both fuels. This result confirms the same engine mechanical behavior, e.g., losses, independent of the burned fuel. From Table 7 it can be concluded that the engine running on E100 rejects less power through cooling and exhaust systems.

According to Razmara *et al.* (2016) the data of Table 7 can be plotted in Sankey diagrams for E22 (Figure 2) and E100 (Figure 3).

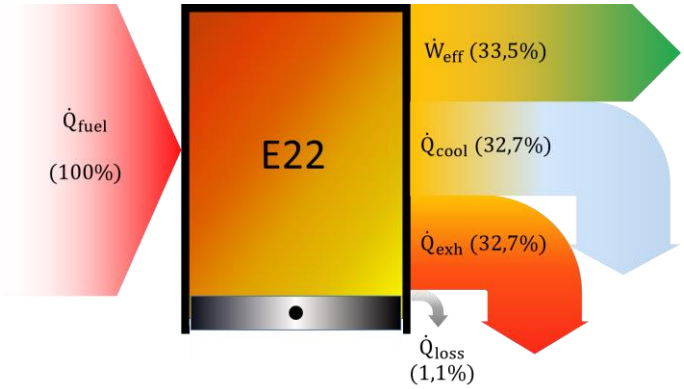

Figure 2: Sankey energy diagram for E22.

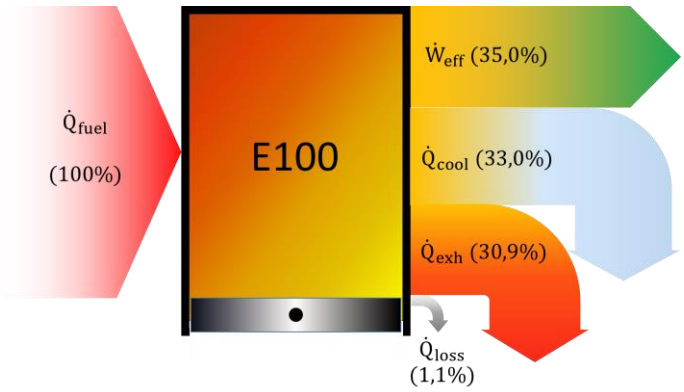

Figure 3: Sankey energy diagram for E100.

The engine energetic efficiency (η_{en}), usually known as global efficiency (η_g), expresses the effective power over the energy from fuel flow, Equation 18.

$$\eta_g = \eta_{en} = \frac{\dot{W}_{eff}}{\dot{m}_{fuel} LHV} \tag{18}$$

The global efficiency of this study is calculated and shown in Table 8. The global efficiency of tested engine resulted about 4.5% higher for the engine running on E100 compared to E22 which is a significant improvement. This advantage can be explained by the higher combustion efficiency of E100 allowing higher power conversion from combustion chamber to engine mechanical output axle.

Table 8. Energetic efficiency (global).

Fuel		**E22**	**E100**	
Engine speed	n	2500	2500	rpm
Mean effective pressure	BMEP	9.09	9.09	bar
Effective power	$\dot{W}_{eff}$	30.3	30.3	kW
Fuel energy flow rate	$\dot{Q}_{fuel}$	90.51	86.63	kW
Global efficiency	**η_g**	**33.48**	**34.98**	**%**

According to the energetic analysis the fuel energy that is not converted in effective mechanical power is rejected to ambient. From this analysis it is not possible to estimate how much energy rejected though engine cooling and exhaust systems could be recovered.

3.2 Exergetic efficiency

The calculation of the amount of the rejected energy that could be effectively recovered is performed by the exergetic analysis. From the exergy concept it is possible to estimate how recoverable is the rejected energy considering that the maximum reuse is limited by Carnot's thermal efficiency.

Similarly to energetic analysis, the classic exergetic analysis is determined according to Equation 19 relating the engine effective power ($\dot{W}_{eff}$) and the fuel exergy ($\dot{B}_{fuel}$).

$$\eta_{exe} = \frac{\dot{W}_{eff}}{\dot{B}_{fuel}} \tag{19}$$

The classic exergetic efficiency (η_{exe}) results from Equation 19 are shown in Table 9 and confirms that for conventional internal combustion engines, like this case study, both efficiencies, energetic and exergetic, are similar, being the fuel exergy the only difference. This classic exergetic efficiency approximates both tested fuels.

Table 9. Exergetic efficiency.

Fuel		**E22**	**E100**	
Engine speed	n	2500	2500	rpm
Mean effective pressure	BMEP	9.09	9.09	bar
Effective power	$\dot{W}_{eff}$	30.3	30.3	kW
Fuel exergy flow rate	$\dot{B}_{fuel}$	97.22	97.25	kW
Exergetic efficiency (classic)	$\boldsymbol{\eta_{exe}}$	**31.17**	**31.16**	**%**

The exergy concept can be more explored determining the destroyed exergy of Equation 2. The destroyed exergy cannot be recovered due to thermodynamic limitations. In this study the exergy rejected through cooling system and through exhaust gases were destroyed.

The exergetic efficiency determined from destroyed exergy concept results the maximum rejected exergy that can be theoretically recovered. This estimation can be considered maximum exergetic efficiency ($\eta_{exe,max}$).

The maximum exergetic efficiency is determined according to Equation 20 (shown in table 10) which considers the fuel exergy and the destroyed exergy.

$$\eta_{exe,max} = \frac{\dot{B}_{fuel} - \dot{B}_d}{\dot{B}_{fuel}} \tag{20}$$

Table 10. Maximum exergetic efficiency.

Fuel		**E22**	**E100**	
Engine speed	n	2500	2500	rpm
Mean effective pressure	BMEP	9.09	9.09	bar
Fuel exergy flow rate	$\dot{B}_{fuel}$	97.22	97.25	kW
Coolant exergy flow rate	$\dot{B}_{cool}$	-7.71	-7.50	kW
Exhaust exergy flow rate	$\dot{B}_{exh}$	-14.10	-12.27	kW
Effective power	$\dot{W}_{eff}$	30.3	30.3	kW
Destroyed exergy flow rate	$\boldsymbol{\dot{B}_d}$	**45.11**	**47.18**	**kW**
Maximum exergetic efficiency	$\boldsymbol{\eta_{exe,max}}$	**53.60**	**51.49**	**%**

According to Oliveira Jr. (2013), the exergy Grassmann diagram of Figure 4 shows the exergetic efficiency verified on tested engine and the maximum exergetic efficiency that can be achieved for this engine running on E22. The Grassmann diagram for E100 is shown in Figure 5.

Running on E22, 46.4% of the total fuel exergy is destroyed. As the tested engine is not equipped with any recovery system, that could be installed both in cooling and in exhaust systems, the destroyed exergy achieves 68.8% of the total fuel exergy (dotted line in Figure 4).

In a similar analysis, running on E100, 48.5% of the total fuel exergy is destroyed. The tested engine, without recovery systems, destroyed 68.8% (dotted line in Figure 5).

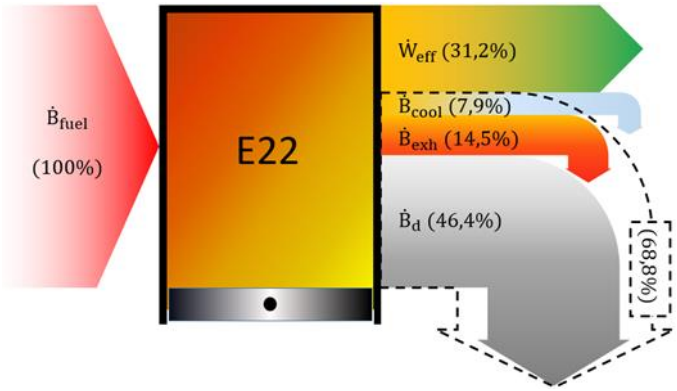

Figure 4: Grassmann exergy diagram for E22.

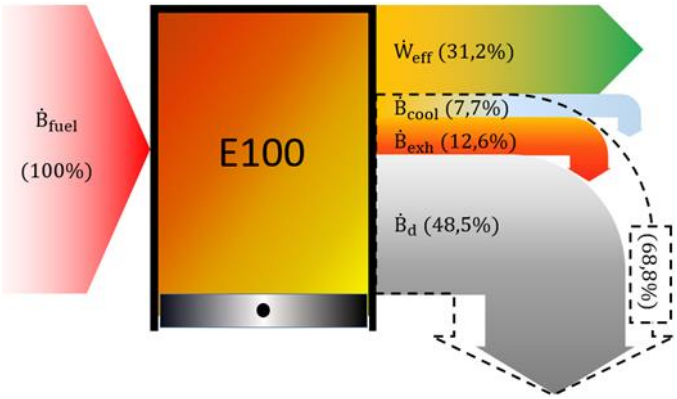

Figure 5: Grassmann exergy diagram for E100.

3.3 A comparison of the Energy and Exergy analysis into a simple engine

A graphical comparison between energetic and exergetic analyses, for both tested fuels, considering the values shown from Figure 2 to Figure 5, is presented in Figure 6. The lower destroyed exergy when running on E22 results in higher exhaust and coolant exergies compared to E100.

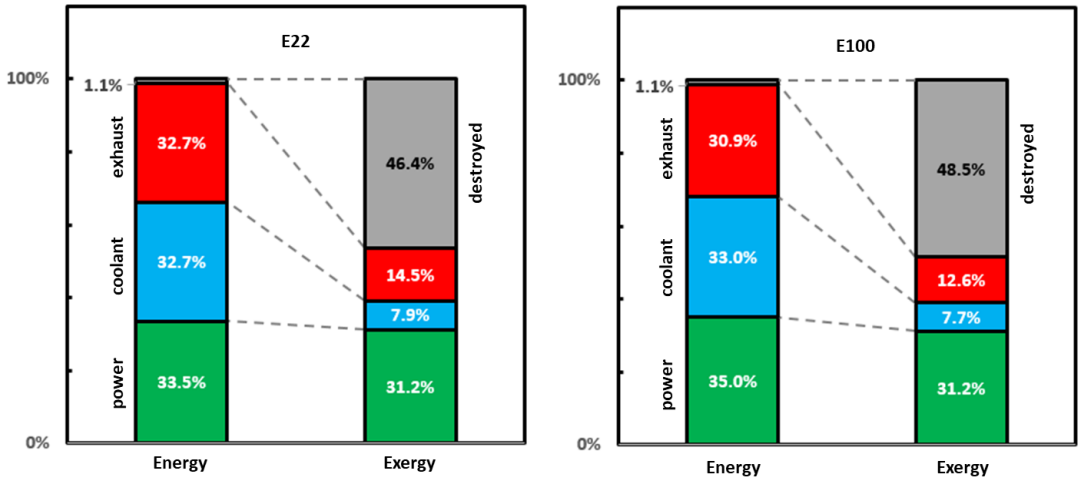

Figure 6: Energy and exergy comparison.

4. CONCLUSIONS

The exergetic analysis allows a realistic comparison of the internal combustion engines against different propulsion technologies. The theoretical higher energetic engine efficiency running on ethanol was confirmed experimentally. The engine achieved 4.5% higher global engine efficiency running on E100 compared to E22. Oppositely, the engine maximum exergetic efficiency running on E22 is 4.1% higher compared to E100. The maximum exergetic efficiency could be theoretically achieved equipping both the engine cooling and exhaust with energy recovery systems operating at Carnot's efficiencies. This analysis points up to 19.77 kW to be recovered with E100 and up to 21.81 kW to be recovered with E22.

5. ACKNOWLEDGEMENTS

The authors would like to acknowledge Centro Universitário FEI and Volkswagen do Brasil for the resources and the opportunity to develop this study.

6. REFERENCES

ANP, 2009, *Resolução ANP No. 38 de 09 de Dezembro de 2009*, Agência Nacional do Petróleo, Gás Natural e Biocombustíveis ANP. DOU 10.12.2009.

ANP, 2015, *Resolução ANP No. 19 de 15 de Abril de 2015*, Agência Nacional do Petróleo, Gás Natural e Biocombustíveis ANP. DOU 17.04.2015.

Chatzopoulou, M.N., and Markides, C.N., 2018. "Thermodynamic optimisation of a high-electrical efficiency integrated internal combustion engine – Organic Rankine cycle combined heat and power system". *Applied Energy*, Vol. 226, pp. 1229-1251, ISSN 0306-2619, https://doi.org/10.1016/j.apenergy.2018.06.022.

De Lima, A.J.T.B., Ruffino, C.H., Ferreira, J.V., and Gallo, W.L.R., 2020. "Study on exergy recovery in hybrid vehicles via wastegate losses". *International Journal of Thermodynamics*, Vol. 23, No. 1, pp. 43-51, https://doi.org/10.5541/ijot.633112.

Heywood, J.B., 1988. *Internal Combustion Engine Fundamentals*. McGraw-Hill, United States of America, ISBN 0-07-028637-X.

INMETRO, 2008, *Vehicle Labeling Conformity Assessment Regulation for Passenger Cars and Light Commercial Vehicles with Otto Cycle Engines* (in Portuguese), Instituto Nacional de Metrologia, Normalização e Qualidade Industrial INMETRO, Rio de Janeiro, www.inmetro.gov.br, Portaria No. 391 de 04 de Novembro de 2008.

Kotas, T.J., 1985. *The Exergy Method of Thermal Plant Analysis*. Butterworths, London, ISBN 0-89464-941-8.

Mahabadipour, H., Srinivasan, K.K., and Krishnan, S.R., 2019. "An exergy analysis methodology for internal combustion engines using a multi-zone simulation of dual fuel low temperature combustion". *Applied Energy*, Vol. 256, 113952, ISSN 0306-2619, https://doi.org/10.1016/j.apenergy.2019.113952.

Moran, M.J., Shapiro, H.N., Boettner, D.D., and Bailey, M.B., 2011. *Fundamentals of Engineering Thermodynamics*. 7th ed., John Wiley & Sons, United States of America, ISBN 13 978-0470-49590-2.

Oliveira Jr., S. de, 2013. *Exergy Production, Cost and Renewability*. Springer-Verlag, London, ISBN 978-1-4471-4165-5, DOI 10.1007/978-1-4471-4165-5.

Özkan, M., 2015. "A Comparative Study on Energy and Exergy Analyses of a CI Engine Performed with Different Multiple Injection Strategies at Part Load: Effect of Injection Pressure". *Entropy*, Vol. 17, No. 1, pp. 244-263, https://doi.org/10.3390/e17010244.

Ranieri, M.A., Manieri, G., Mady, C.E.K., and Albuquerque, C., 2018. "Analysis of an absorption refrigeration system for air-conditioning of a microbus". In *Proceedings of the 31st International Conference on Efficiency, Cost, Optimization, Simulation and Environmental Impact of Energy Systems - ECOS 2018*. Guimarães, Portugal.

Razmara, M., Bidarvatan, M., Shahbakhti, M., and Robinett, R.D., 2016. "Optimal exergy-based control of internal combustion engines". *Applied Energy*, Vol. 183, pp. 1389-1403, ISSN 0306-2619, https://doi.org/10.1016/j.apenergy.2016.09.058.

Ruffino, C.H., De Lima, A.J.T.B., Mattos, A.P., Allah, F.U.M., Bernal, J.L.L., Ferreira, J.V., and Gallo, W.L.R., 2019. "Exergetic analysis of a spark ignition engine fuelled with ethanol". *Energy Conversion and Management*, Vol. 192, pp. 20-29, ISSN 0196-8904, https://doi.org/10.1016/j.enconman.2019.04.035.

Szargut, J., Morris, D. R., and Steward, F. R., 1988. *Exergy analysis of thermal, chemical and metallurgical processes.* Hemisphere Publishing Corporation, United States of America, ISBN 0-89116-574-6.

7. RESPONSIBILITY NOTICE

The authors are the only responsible for the printed material included in this paper.